

# GARSTEC—the Garching Stellar Evolution Code

## The direct descendant of the legendary Kippenhahn code

Achim Weiss · Helmut Schlattl

Received: 18 April 2007 / Accepted: 20 July 2007 / Published online: 15 August 2007  
© Springer Science+Business Media B.V. 2007

**Abstract** We describe the Garching Stellar Evolution Code. General features, treatment of the microphysics, details of the numerical solution, handling and particularities are discussed. The standard solar model serves as the most basic benchmark to test the accurateness of the code and is presented, too.

**Keywords** Methods: numerical · Stars: evolution · Sun: evolution

**PACS** 97.10.Cv · 96.60.Jw

## 1 Introduction

Although there is a large number of stellar evolution codes available for modeling stars, many of them can be traced back to a handful of original programs created in the late 1960s or early 1970s of the last century. One of the first numerical programs to solve the stellar structure equations for a complete star is that written by Kippenhahn et al. (1967). This program has been in use at the Max-Planck-Institut für Astrophysik in Garching since then, and has been developed continuously by a number of people. Thomas (1967) improved the physics of high densities and several numerical aspects. In the 1980s A. Weiss modified the treatment of nuclear reactions, opacities and the equation of state (Weiss

1989), and later-on J. Wagenhuber took care of improved numerical stability (Wagenhuber and Weiss 1994), which allowed smooth calculations of thermal pulses on the Asymptotic Giant Branch as well as of the core helium flash in low-mass stars. He also applied the implicit solver scheme (see below) to the whole star, removing the explicit envelope integrations, which were one of the major aspects of the original code (Kippenhahn et al. 1967). Finally, H. Schlattl implemented atomic diffusion and the simultaneous solution of burning and mixing events. The present version has been described most completely by Weiss and Schlattl (2000).

The code is a general purpose stellar evolution code allowing the calculation of stellar models from the pre-main sequence into the early white dwarf stage for low and intermediate masses, and into carbon burning for high masses. On the other hand it is also suited for specific cases that require high accurateness, as the Standard Solar Model, which will be discussed in Sect. 4. In the next section we will discuss the numerical aspects of our code, which we also call GARSTEC. Section 3 will then contain the treatment of physics.

## 2 Numerics

GARSTEC is written in FORTRAN; the core is still FORTRAN 77, but all newer or updated routines are in FORTRAN 90/95. We are complying in most parts to the standard ANSI language definition, such that the code runs on many platforms. With the code we provide utilities for optimized compilation for Intel or other Linux-compilers, IBM, Tru64, SUN and SGI UNIX'es. The flexibility of the code in terms of treatment of physical aspects necessitates also pre-compilation; for example, different table and code packages

---

A. Weiss (✉) · H. Schlattl  
Max-Planck-Institut für Astrophysik, Karl-Schwarzschild-Str. 1,  
85748 Garching, Germany  
e-mail: aweiss@mpa-garching.mpg.de

H. Schlattl  
e-mail: helmut.schlattl@gsf.de

for the equation of state are included depending on pre-compiler options.

Some auxiliary routines, concerned with string handling and the setting of system variables, are written in C. The code needs of order 200–300 MB and runs with acceptable speed on present-day generations of PCs. Disk-I/O is kept to a minimum by storing previous models, which may be needed for back-stepping in case of lacking convergence, in memory. Processor usage is always above 95%. Disk space requirements depend on the amount of stored results and log-files. It can be anywhere between 150 MB and several 10 GB.

The pre-1990s version of the code is documented in an unpublished manual (Weiss 1989), which still contains valuable details about many routines. Schlattl (2004, unpublished) has added an introduction to the code structure, its handling and the associated utilities (e.g. graphical analysis tools). The latter documentation comes with the distribution package of the code, which is freely available from the authors. Otherwise many routines contain in-line documentation (comments), which are helpful for understanding the coding. A complete documentation with descriptions of all subroutines, however, is missing.

## 2.1 Implicit scheme

At the core of GARSTEC is the usual Henyey-scheme (Henyey et al. 1964, 1965) for solving the four standard structure equations on a discretized grid. Details of the implementation were discussed also in the Kippenhahn–Weigert textbook (Kippenhahn and Weigert 1990), chapter 11.2. The Henyey solver therefore solves a system of  $8 \times 4$  block matrices throughout the star. However, for solving problems which contain 2nd or higher order derivatives, as they appeared with the introduction of diffusion, we have extended the standard Henyey-solver, which is now flexible in terms of the number of equations and variables. The difference equations are formulated in first order with centered arithmetic mean values of the variables, except for strongly varying variables (e.g. energy generation), for which geometric means are used.

Derivatives of the equations are calculated analytically, but those of physical quantities appearing in the equations are usually obtained from numerical differentiation using fixed increments in the variables, the size of which is chosen as being typical for the case of good convergence (e.g.  $\Delta \log T = 10^{-4}$ ).

The Lagrangian variable is relative mass ( $M_r/M$ ) throughout the star, i.e. up to the photosphere, with a minimum increment of  $10^{-13}$ ; the resolution is flexible, depending on the run of physical variables, but also on the accurateness of the solution of the differential equations (details on this “gradient method” can be found in Wagenhuber and

Weiss 1994). In short, we compute at a gridpoint  $x_0$  the quantity

$$\left| f(x_0 + \xi) - \left( f(x_0) + \left. \frac{df(x)}{dx} \right|_{x_0} \xi \right) \right| < \delta, \quad (1)$$

where  $\xi$  is the increment in  $x$ , which must be small enough to ensure the above accuracy condition, with  $\delta = 10^{-4}$ – $10^{-3}$  typically.  $f$  is any structure variable.  $\xi$  can be estimated to be (Wagenhuber and Weiss 1994)

$$\xi \approx (x_1 - x_0) \sqrt{\frac{\delta}{|3(f_1 - f_0) - (f'_1 + 2f'_0)(x_1 - x_0)|}}. \quad (2)$$

This ensures that the linear approximation actually used in the grid resolution is accurate to the level  $\delta$ . One can then compare the actual grid-step ( $x_1 - x_0$ ) with  $\xi$  (for all variables) and accordingly insert or remove grid points. This method assures that in regions of strongly varying gradients grid points are inserted, while in areas of almost linear behaviour of the structural variables unnecessary points are removed. We typically use of order 500–1000 grid points for a main sequence model, 1500 for a red giant, and 3000 during short-lived energetic episodes like core helium flash and thermal pulses. Our standard solar model has about 1900 grid points due to the enhanced accuracy requirement.

Thanks to this grid control scheme it became possible to routinely calculate low-mass models through the core helium flash, and to follow intermediate-mass models along the thermally pulsing Asymptotic Giant Branch.

Convergence control is done by checking the corrections to all four structure variables throughout the complete model applied in each iteration. The structure variables are  $\log P$ ,  $\log T$ ,  $\log r$ , and  $L_r/L$ . The transformation between physical quantity and actual Lagrangian and structure variables used in the code can in fact be changed, e.g. to the traditional  $\log(1 - M_r/M)$ . To deal with the deficits of a simple first-order Newton iteration scheme, the code analyzes the progress or lack of convergence and applies the calculated corrections only partially; this *undercorrection factor* can be as low as 0.001 but also larger than unity.

Boundary conditions are the usual regularity conditions at the center, and the Stefan–Boltzmann law at the surface (photosphere) together with the pressure–radius relation obtained from integrating a massless grey Eddington atmosphere. Alternatively, external atmospheres can be used, from which the lower boundary is taken as the outer boundary condition for the stellar interior.

## 2.2 Explicit time integration

Time-dependent equations concerning the composition changes inside the star (nuclear burning, diffusive and other mixing processes) are solved between two interior models

by integrating them over an *evolutionary timestep*, split up into several (typically 10–20) smaller *nuclear timesteps*. The standard procedure is to keep  $T$ ,  $P$  and/or  $\rho$  constant over the whole evolutionary timestep, which in general underestimates the true temperature and density evolution. We alternatively have at hand a second order predictor-corrector scheme for  $T(t)$  and  $\rho(t)$  which leads to a higher accuracy of the time evolution, but requires additional iterations in time between two successive models. We find that in general the predictor-corrector scheme is more accurate and allows larger timesteps, but that the net gain is not significant compared to the standard scheme with appropriately smaller timesteps.

The terms  $\partial T/\partial t$  and  $\partial P/\partial t$  appearing in the energy equation ( $\varepsilon_g$ ) are treated in first order in the implicit scheme, keeping  $\Delta t$  (the last evolutionary timestep) and  $P(t_0)$  and  $T(t_0)$  of the previous model constant and solving only for  $P(t_0 + \Delta t)$  and  $T(t_0 + \Delta t)$ . We have recently implemented a second-order scheme, but do not find a significant influence on code performance or accuracy.

Optionally, the acceleration term  $\partial^2 r/\partial t^2 = \partial v/\partial t$  in the pressure equation can be considered by using the additional equation for the shell velocity  $v = \partial r/\partial t$ , which is implemented in GARSTEC. The time derivatives are calculated in first order only using the radius and shell velocity of the previous models. When the acceleration term is neglected, its value is computed from the radius changes in the previous two models for diagnostic purposes to see how well the hydrostatic assumption is fulfilled.

### 2.3 Interpolation schemes

Since both the equation of state (EoS) as well as the opacities are used as tables, interpolation within and between tables is necessary. For many input physics tables we are using the two-dimensional, bi-rational spline algorithm of Spaeth (1973). This method contains free parameters for the two coordinates, which determines whether the interpolant is close to a cubic or a linear function, which, independent of the parameter, always remains twice differentiable. This allows to reproduce step-like behaviour in tables very accurately without the usual spline oscillations. Although these parameters can be chosen for each table cell individually, we use one number for the whole table. We select a value (1–3), which is equivalent to a very moderate damping of the cubic spline. The spline interpolation also yields the derivatives necessary for the implicit Henyey-solver. If we have to interpolate between tables for the appropriate composition, we use straightforward parabolic interpolation (see Sect. 3.2.4).

### 2.4 Calculation of initial models

Although in general pre-existing models are used for new sequences (initial mass and composition can be reset and

modified), a 4th order Runge–Kutta solver is available to create new models from scratch. The composition of the new model does not need to be homogeneous. This allows not only the calculation of pre- and zero-age main sequence, but also of zero-age horizontal branch models.

When a previous model is used as a new starting model on the ZAMS, and mass and/or composition are changed, the chemical evolution as well as the thermal energies are suppressed and the model recalculated several times to allow the adjustable grid to relax.

## 3 Physics details

### 3.1 General considerations

#### 3.1.1 Basic assumptions

The code is one-dimensional, hydrostatic (except for the optional inclusion of the acceleration term in the pressure equation), and does not include effects of rotation. In the standard version, convective mixing is instantaneous, and we ignore overshooting and semiconvection. In all three aspects the code can optionally include these effects, but has not been calibrated thoroughly to determine best-choice values for the respective parameters.

#### 3.1.2 Atmosphere

We routinely use a plane-parallel Eddington grey atmosphere with realistic (but always Rosseland mean) opacities. Optionally, the Krishna-Swamy  $T$ – $\tau$ -relation (Swamy 1966) can be employed. Both are fitted to the interior at  $\tau = 2/3$ . We have also implemented the Lucy (1976) spherical atmosphere, which can contain mass (this can be important for AGB models). The code is also prepared for accepting any outer boundary condition from any more realistic atmosphere at any optical depth (Schlattl et al. 1997).

#### 3.1.3 Mass loss

Mass loss is always treated according to analytical and explicit formulae (such as the Reimers formula) and applied between two subsequent models. Total mass is reduced accordingly. The number of grid points remains constant, as do the values for the independent structure variables. However, the (absolute) mass assigned to the grid points is rescaled (stretched) down to some pre-defined value to take into account that the deeper interior is unaffected by the mass loss, and the drop of pressure and temperature between core and photosphere remains similar (after adjustment), but covers a narrower envelope mass range.

### 3.1.4 Elements and isotopes

The code knows of 64 elements and isotopes from  $^1\text{H}$  to  $^{56}\text{Ni}$ . However, different parts of the program take only subsets of these into account. The opacity package, for example, considers only the hydrogen and metal mass fractions  $X$  and  $Z$ . It must therefore be ensured that relative metal fractions (usually solar-scaled or  $\alpha$ -enhanced) have been used for the calculations of the opacity tables, which are consistent with the stellar mixture (apart from smaller variations such as the CN-conversion in CNO-burning). The equation of state has the same restriction.

Atomic diffusion considers 13 elements and isotopes from hydrogen to iron; this list is almost the same as that in the nuclear network (Sect. 3.2.1).

### 3.1.5 Convection

We use standard mixing-length theory in the formulation of (Kippenhahn and Weigert 1990);  $\alpha_{\text{MLT}}$  is usually close to the “calibrated” one obtained from the standard solar model ( $\alpha_{\text{MLT}} \approx 1.6$ – $1.8$ ). Alternatively, the *Full Turbulent Spectrum Theory* by Canuto and Mazzitelli (1992) is implemented, again with a free parameter (with a “calibrated” solar parameter of order 0.9). Either the Schwarzschild- (standard) or Ledoux-criterion can be used. A grid cell is considered to be convectively unstable, if  $\nabla_{\text{rad}} > \nabla_{\text{ad}}$  at both cell edges, i.e., grid points. If the mixing is treated non-instantaneous (optionally), we treat it as a diffusive process with a typical convective velocity  $v_c$  estimated from mixing-length theory. The cubic equation of MLT is solved with a Newton-iteration, since the analytical solution is numerically inaccurate for high superadiabaticity.

Similarly, convective overshooting is considered to be a diffusive process. We use the description by Freytag et al. (1996), with a diffusion constant

$$D(z) = D_0 \exp \frac{-2z}{fH_P}, \quad (3)$$

where  $f$  is a free constant ( $f = 0.016$  as the standard value) and  $H_P$  the usual pressure scale height.  $z$  is the radial distance from the formal Schwarzschild border, and  $D_0$  sets the scale of diffusive speed and is derived from the MLT-convective velocity.

Semiconvection has been implemented, again as a diffusive process, but not been tested nor used so far.

### 3.1.6 Diffusion

Atomic diffusion is applied between two consecutive models, as are all other changes with time. The diffusion coefficients are calculated following the prescription in Thoul et al. (1994); elements considered are either hydrogen and

helium only, or any selection of metals in addition. In the latter case, the proper diffusive speed of each element is considered. No radiative levitation is taken into account.

While in the standard treatment of diffusion, all elements are assumed to be fully ionized, an extension of the diffusion treatment (Schlattl 2002) is available which considers the actual ionization stage of each element (if this information is provided by the EoS). Furthermore, more accurate diffusion constants can be computed from improved collision integrals with additional quantum corrections (Schlattl and Salaris 2003).

The system of second order differential equations is solved on the same spatial grid as the structure equations with the extended Henyey-solver. As the equations are fairly general, other diffusive effects like time-dependent convective mixing, overshooting, extra-mixing, etc., can be included in the same scheme.

## 3.2 Microphysics

### 3.2.1 Nuclear reactions

The nuclear reaction rates are either from the NACRE cooperation (Angulo et al. 1999), or from the compilations by Fowler and coworkers (Caughlan et al. 1985; Caughlan and Fowler 1988). In all cases we use the analytical approximations provided. For hydrogen reactions in solar models the program also employs the recommended rates by Adelberger et al. (1998). The crucial reaction rate  $^{12}\text{C}(\alpha, \gamma)^{16}\text{O}$  is taken from (Kunz et al. 2002). Screening is treated in general in the weak limit, following Salpeter’s classical formula (Salpeter 1954).

The nuclear reactions are followed by a small network that treats (as the default) either H-burning or He- and higher burning separately. The nuclei explicitly considered are  $p$ ,  $^3\text{He}$ ,  $^4\text{He}$ ,  $^{12}\text{C}$ ,  $^{13}\text{C}$ ,  $^{14}\text{N}$ ,  $^{15}\text{N}$ ,  $^{16}\text{O}$ , and  $^{17}\text{O}$ , respectively  $p$ ,  $n$ ,  $^4\text{He}$ ,  $^{12}\text{C}$ ,  $^{16}\text{O}$ ,  $^{20}\text{Ne}$ ,  $^{24}\text{Mg}$ ,  $^{28}\text{Si}$ , and  $^{56}\text{Ni}$ . The treatment of burning phases beyond He-burning is therefore very rudimentary.

If needed, the nuclear network can treat both H- and He-burning simultaneously. Since this is usually connected with very short timescales and violent convection, in this case convective mixing is automatically dealt with in the diffusive, non-instantaneous way.

The network is solved by an implicit backward-differencing scheme of the linearized equations. Therefore special care has to be taken of the nuclear timesteps (see Sect. 2.2), which are controlled by keeping abundance changes at a level of 10% per step.

For both the purpose of following the evolution of the chemical species and the nuclear energy production during the solution of the spatial problem we use the same nuclear network. However, for the nuclear energy production

the abundance changes are computed with the present abundances, temperature and density, i.e. in an explicit rather than in an implicit way. From the abundance changes the mass changes can be computed using the appropriate atomic masses and finally the energy production rate is obtained. This provides a snapshot of the energy production. A comparison of this value with the average energy output of the following time-step serves as an additional quality parameter for the chemical evolution, which can also be applied as a criterion to limit the evolutionary timestep.

Alternatively, one could solve the full nuclear network by the implicit method for the present abundance changes. These are then converted to energy output by computing the net change of binding energies. For the nuclear energy production, the abundance changes are determined from the current composition in the model, using a nuclear timestep of 1% of the last evolutionary one. This method has been used when the nuclear network was designed, but is presently disabled.

Both methods to compute the nuclear energy generation do not include energy losses by neutrinos; we add them separately using the numbers given in the sources for the reaction rates.

We stress that the reduction in stellar mass due to nuclear reactions is taken into account in our code.

### 3.2.2 Neutrino losses

In addition to neutrino losses during nuclear processes, which are taken care of in the nuclear network, neutrinos produced in the hot and dense plasma serve as an energy sink. We use the fitting formulae by Itoh and coworkers (Munakata et al. 1985), except for plasma neutrinos, where we prefer that by Haft et al. (1994).

### 3.2.3 Thermal energies

A standard way of calculating the gravothermal energies  $\varepsilon_g$  in stellar evolution theory is to use the approximative formula by Kippenhahn and Weigert (1990),

$$\varepsilon_g = -T \frac{\partial s}{\partial t} = -c_P \frac{\partial T}{\partial t} + \frac{\delta}{\rho} \frac{\partial P}{\partial t}. \quad (4)$$

However, this formula ignores changes in entropy and molecular weight due to composition changes (“mixing entropy”), which may contribute in regions of nuclear energy production or moving convective boundaries. Only in the latter this effect may be needed. The exact formula for  $\varepsilon_g$  implemented in the code is

$$\varepsilon_g = -\frac{\partial u}{\partial t} + \frac{P}{\rho^2} \frac{\partial \rho}{\partial t}, \quad (5)$$

where  $u$  is the specific internal energy. For the higher precision of solar models we always use it instead of (4).

### 3.2.4 Opacities

Our code uses tables of Rosseland mean opacities  $\kappa$  for mixtures quantified by the mass fractions of hydrogen and metals (both ranging from 0 to 1; the total number of tables is of order 80), and with a temperature and density grid of about 85 and 25 grid points. As the density coordinate we actually use the usual  $\log R = \log \rho - 3 \log T + 18$ . The interpolation in this grid is done by the mentioned two-dimensional, bi-rational spline algorithm, and in mixture we use parabolic polynomials first in  $X$  (hydrogen) between the three tables closest to the actual value, and then in  $\log Z$  (metallicity). In practice, and as long as the total metallicity is not changing, e.g. either by advanced nuclear burning phases or metal diffusion, tables for only three metallicity values are sufficient for the whole calculation. For evolutionary stages from core helium burning on, we have special core tables.

The tables themselves are the end product of the merging of various data sources. We have four main regions in the  $T$ – $R$  domain:

- $\log T < 3.8$ , for which we use the Wichita State Alexander & Ferguson molecular opacity tables (Alexander and Ferguson 1994; Ferguson et al. 2005).
- $4.1 < \log T < 8.7$ , for which OPAL tables are used (Iglesias and Rogers 1996).
- High density: here we employ the results by Itoh et al. (1983) for electron conduction opacities.
- $\log T > 8.7$ , for which no OPAL data are available; here we use the old Los Alamos Opacity Library (Huebner et al. 1977).

In between these regions are transitions. Between  $3.8 < \log T < 4.1$ , where both Wichita State and OPAL data are available, we have a linear transition in  $\log \kappa$  along with  $\log T$  from one source to the other. The agreement between both tables is excellent and the transition is very smooth. At the high-density edge we add radiative ( $\kappa_r$ ) and conductive ( $\kappa_c$ ) opacities according to

$$1/\kappa = 1/\kappa_r + 1/\kappa_c.$$

Since with increasing density electron conduction is dominating the transport of energy, the radiative contribution can be omitted once  $\kappa_r > \kappa_c$ . However, in particular at  $\log T < 5$  the radiative tables end before this situation is reached. In case the gap between the end of the radiative opacity table and the density from which on  $\kappa_c$  is already lower than the last radiative value available is only 1–2 dex, we boldly interpolate over this gap (cubic spline). If the gap is too large, the final  $\kappa$ -table has to end here. Should we run out of the table definition range during the stellar model calculations, we use the last table value. This happens at isolated points in some low-mass main-sequence envelopes and cannot be

avoided as long as the input tables do not cover the full  $\rho$ - $T$ -plane.

All our tables are constructed in this same way in a separate step before they are used by the stellar evolution code. In fact, the calculation of the spline coefficients is the last step in the preparation of the tables, such that the stellar evolution code reads only these coefficients and the appropriate parameter for the generalized spline function.

### 3.2.5 Equation of state

The original EoS in the Kippenhahn-code included an ideal gas with radiation pressure and partial ionization of hydrogen and helium. For higher densities partial and full degeneracy was included according to analytical approximation formulae (Kippenhahn and Thomas 1964). These were improved to higher order accuracy by Wagenhuber (1996). The ionization of carbon was included in Weiss (1987) and the solver scheme for the sets of Saha-equation was changed to a Newton-type one. While this EoS is still implemented, it is only used in case that the more modern tabular equations of state do not cover the parameter range (in  $T$  and  $P$ , our EoS input variables).

We preferentially use the OPAL-EoS (Rogers et al. 1996), where different generations of tables have been obtained from the website <http://www-phys.llnl.gov/Research/OPAL>. We prefer the *EOSPLUS* set, i.e. the denser grid tables, which leads to less convergence problems. The latest tables (*EOS\_2001*) are also available. Interpolation in all tables is done by a smoothed quadratic interpolation on a grid of  $4 \times 4$  table values following the OPAL recommendations. Between mixtures we interpolate parabolically. The MHD EoS (Mihalas et al. 1988) is available, too, and was used mainly for solar model calculations, extending the OPAL EoS, when needed.

We recently also implemented Irwin's EoS (Cassisi et al. 2003)<sup>1</sup> in the form of pre-calculated tables. In this case interpolation is done with the same generalized two-dimensional spline method discussed already in Sects. 2 and 3.2.4.

Finally, an (unpublished) EoS (Weiss 1999) consisting of the merging of OPAL-tables, the Saumon–Chabrier EoS (Saumon et al. 1995), and that by Pols et al. (1995) has been developed; it is available for pure H/He-mixtures only due to the restriction of the Saumon–Chabrier tables. The choice between all these EoS table sets is done before compilation as a pre-compiler option.

## 4 The GARSOM Standard Solar Model

The Garching Standard Solar Model (GARSOM) has been developed and published by Schlattl et al. (1997, 1999),

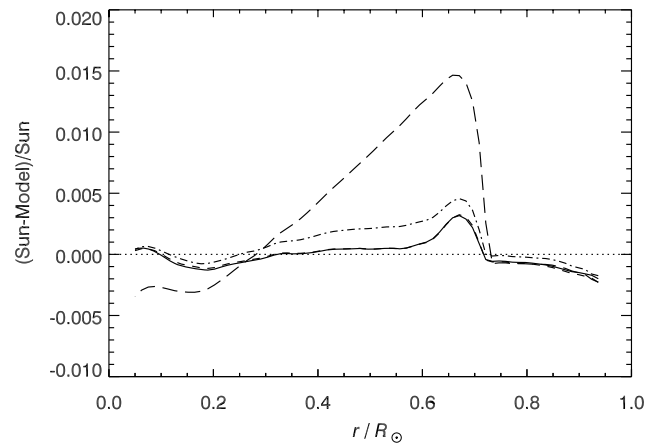


**Fig. 1** Sound speed profiles (relative deviations from the seismic sound speed by Basu and Antia 1997) for the models GARSOM4 (solid), GARSOM41-2 (short-dashed), GARSOM5-1 (dash-dotted) and GARSOM5-3 (long-dashed) of Table 1

and was also used in Bahcall et al. (2005b) for comparison with the Bahcall & Pinsonneault models. In the Garching publications, the OPAL & Alexander opacities for the solar mixture of Grevesse and Noels (1993), the corresponding OPAL EoS, diffusion as in Sect. 3.1.6, and standard MLT were used. These choices also comprise the standard set of physics treatment in GARSTEC. For several solar models FST convection was employed, too. In addition, we sometimes use full 2d-hydro atmospheric models as in Schlattl et al. (1997) for the outer boundary condition.

In the following we present several of these standard solar models. We have calculated them for the Grevesse and Sauval (1998) as well as for the Asplund et al. (2005) new solar composition. We use standard MLT and FTS convection theory, and employ OPAL and Irwin-EoS. H-, He-, and metal diffusion is always fully accounted for, but with different methods for calculating the diffusive speeds (see Sect. 3.1.6).

It can easily be seen from the values in the table and the sound speed profile that the main influence comes from the  $(Z/X)_s$  calibration, i.e. the total metallicity, while the distribution of metals (GN93, GS98, or AGS04) does not affect the solar structure. This is particularly evident from comparing GARSOM4 with GARSOM41-2; the two sound speed profiles (Fig. 1; solid and short-dashed lines) can be discriminated only for  $r/R_\odot < 0.35$  and  $r/R_\odot > 0.85$ . The latter difference can be explained by the fact that GARSOM4 uses the 2d-hydro atmospheres, which leads to different values of  $\alpha_{\text{conv}}$ , too.

## 5 Summary

We have introduced GARSTEC, the “Garching Stellar Evolution Code”, and sketched its main features and the treat-

<sup>1</sup> Available from <http://freeeos.sourceforge.net/>

**Table 1** Global quantities of various GARSOM Standard Solar models. All models match the solar  $\log L$  and  $\log T_{\text{eff}}$  (taken here as 5780 K) constraint to better than  $10^{-4}$ , and that of the measured  $(Z/X)_s$  to 1%.  $\alpha_{\text{conv}}$  is the free parameter of the convection model employed,  $R_{\text{bcz}}/R_{\odot}$  the depth of the convective zone. TBL stands for (H/He/metal-) diffusion a la Thoul et al. (1994), and QSchl if the improvements by Schlattl (Schlattl and Salaris 2003; Schlattl 2002) are included. The column “Comp.” gives the source for internal metal ratios in the model composition, while “Opac.” contains that of the

opacity tables used. GARSOM41-1 and -2 models were calibrated to  $Z/X = 0.0245$  (Grevesse and Noels 1993, GN93), although they use (composition and opacity tables) the GS98 metal ratios. The column “Atm.” indicates whether gray Eddington (EG), Krishna-Swamy (KS), or 2-d hydro atmospheres (2d) were used for the outer boundary conditions. Additionally, two reference models from Bahcall et al. (2005a) are added, which should be compared to GARSOM41-1 (BP04) and GARSOM5-3 (BS05)

Model	Comp.	Conv.	Opac.	EOS	Diff.	Atm.	$Y_i$	$Z_i$	$\alpha_{\text{conv}}$	$R_{\text{bcz}}/R_{\odot}$	$Y_s$	$(Z/X)_s$
GARSOM4	GN93	FST	GN93	OPAL	TBL	2d	0.2746	0.0199	0.975	0.7133	0.2448	0.02450
GARSOM41-1	GS98	MLT	GS98	OPAL	TBL	EG	0.2753	0.0200	1.741	0.7134	0.2453	0.02450
GARSOM41-2	GS98	FST	GS98	OPAL	TBL	EG	0.2754	0.0200	0.899	0.7133	0.2452	0.02456
GARSOM5-1	GS98	FST	GS98	Irwin	QSchl	2d	0.2695	0.0188	0.898	0.7151	0.2409	0.02300
GARSOM5-2	AGS04	FST	GS98	Irwin	QSchl	2d	0.2447	0.0141	0.840	0.7278	0.2165	0.01650
GARSOM5-3	AGS04	FST	AGS04	Irwin	QSchl	2d	0.2599	0.0139	0.912	0.7302	0.2297	0.01650
BP04	GS98	MLT	GS98	OPAL	TBL	KS	0.2734	0.0188	2.07	0.7147	0.243	0.0228
BS05	AGS04	MLT	AGS04	OPAL	TBL	KS	0.2614	0.0140	1.96	0.7289	0.230	0.0165

ment of all physical aspects. Although the code is a historically grown one, modified by generations of students and scientists at the Max-Planck-Institut für Astrophysik in Garching, it is nevertheless fully up-to-date. Its main advantages are the highly modular program structure, the fully implicit scheme for the spatial problem, and the possibility to solve nuclear burning and mixing processes simultaneously. It can be used for a large mass range and most phases of stellar evolution. Nevertheless, great efforts have been undertaken to ensure high accurateness, such that also the requirements imposed by seismology can be matched.

## References

- Adelberger, E., Austin, S., Bahcall, J., Balantekin, A., Bogaert, G., Buchmann, L.: Solar fusion cross sections. *Rev. Mod. Phys.* **70**, 1265–1291 (1998)
- Alexander, D.R., Ferguson, J.W.: Low-temperature Rosseland opacities. *Astrophys. J.* **437**, 879–891 (1994)
- Angulo, C., Arnould, M., Rayet, M., et al.: A compilation of charged-particle induced thermonuclear reaction rates. *Nucl. Phys. A* **656**, 3–183 (1999)
- Asplund, M., Grevesse, N., Sauval, A.J.: The solar chemical composition. In: Barnes, T.G. III, Bash, F.N. (eds.) *Cosmic Abundances as Records of Stellar Evolution and Nucleosynthesis*. ASP Conf. Ser., vol. 336, pp. 25–38 (2005)
- Bahcall, J., Serenelli, A., Basu, S.: New solar opacities, abundances, helioseismology, and neutrino fluxes. *Astrophys. J.* **621**, L85–L88 (2005a)
- Bahcall, J.N., Basu, S., Pinsonneault, M., Serenelli, A.M.: Helioseismological implications of recent solar abundance determinations. *Astrophys. J.* **618**, 1049–1056 (2005b)
- Basu, S., Antia, H.M.: Seismic measurement of the depth of the solar convective zone. *Mon. Not. Roy. Astron. Soc.* **287**, 198 (1997)
- Canuto, V., Mazzitelli, I.: Further improvements of a new model for turbulent convection in stars. *Astrophys. J.* **389**, 724–730 (1992)
- Cassisi, S., Salaris, M., Irwin, A.: The initial helium content of galactic globular cluster stars from the R-parameter: comparison with the cosmic microwave background constraint. *Astrophys. J.* **588**, 862–870 (2003)
- Caughlan, G., Fowler, W.: Thermonuclear reaction rates V. *At. Data Nucl. Data Tables* **40**, 283–334 (1988)
- Caughlan, G., Fowler, W., Harris, H., Zimmerman, B.: Tables of thermonuclear reaction rates for low-mass nuclei ( $1 \leq z \leq 14$ ). *At. Data Nucl. Data Tables* **32**, 197–233 (1985)
- Ferguson, J.W., Alexander, D.R., Allard, F., Barman, T., Bodnarik, J.G., Hauschildt, P.H., Heffner-Wong, A., Tamanai, A.: Low-temperature opacities. *Astrophys. J.* **623**, 585–596 (2005)
- Freytag, B., Ludwig, H.-G., Steffen, M.: Hydrodynamical models of stellar convection. *Astron. Astrophys.* **313**, 497–516 (1996)
- Grevesse, N., Noels, A.: Atomic data and the spectrum of the solar photosphere. *Phys. Scripta T* **47**, 133–138 (1993)
- Grevesse, N., Sauval, A.: Standard solar composition. *Space Sci. Rev.* **85**, 161–174 (1998)
- Haft, M., Raffelt, G., Weiss, A.: Standard and nonstandard plasma neutrino emission revisited. *Astrophys. J.* **425**, 222–230 (1994). Erratum: **438**, 1017 (1995)
- Heney, L.G., Forbes, J.E., Gould, N.L.: A new method of automatic computation of stellar evolution. *Astrophys. J.* **139**, 306–317 (1964)
- Heney, L., Vardya, M.S., Bodenheimer, P.: Studies in stellar evolution. III. The calculation of model envelopes. *Astrophys. J.* **142**, 841–854 (1965)
- Huebner, W.F., Merts, L., Magee, N.H. Jr., Argo, M.F.: Astrophysical opacity library. Scientific Report LA-6760-M, Los Alamos Scientific Laboratory (1977)
- Iglesias, C.A., Rogers, F.J.: Updated OPAL opacities. *Astrophys. J.* **464**, 943–953 (1996)
- Itoh, N., Mitake, S., Iyetomi, H., Ichimaru, S.: Electrical and thermal conductivities of dense matter in the liquid metal phase. I—High-temperature results. *Astrophys. J.* **273**, 774–782 (1983)
- Kippenhahn, R., Thomas, H.-C.: Integralapproximationen für die Zustandsgleichung eines entarteten Gases. *Z. Astrophys.* **60**, 19–23 (1964)
- Kippenhahn, R., Weigert, A.: *Stellar Structure and Evolution*. A&A Library. Springer, Heidelberg (1990)

- Kippenhahn, R., Weigert, A., Hofmeister, E.: Methods for calculating stellar evolution. *Meth. Comp. Phys.* **7**, 129–190 (1967)
- Kunz, R., Fey, M., Jaeger, M., Mayer, A., Hammer, J.W., Staudt, G., Harissopulos, S., Paradellis, T.: Astrophysical reaction rate of  $^{12}\text{C}(\alpha, \gamma)^{16}\text{O}$ . *Astrophys. J.* **567**, 643–650 (2002)
- Lucy, L.B.: Mass loss by cool carbon stars. *Astrophys. J.* **205**, 482–491 (1976)
- Mihalas, D., Däppen, W., Hummer, D.G.: The equation of state for stellar evolution II. *Astrophys. J.* **331**, 815–825 (1988)
- Munakata, H., Kohyama, Y., Itoh, N.: Neutrino energy loss in stellar interiors. *Astrophys. J.* **296**, 197 (1985). Erratum: **304**, 580 (1986)
- Pols, O.R., Tout, C.A., Eggleton, P.P., Han, Z.: Approximate input physics for stellar modelling. *Mon. Not. Roy. Astron. Soc.* **274**, 964–974 (1995)
- Rogers, F.J., Swenson, F.J., Iglesias, C.A.: OPAL equation-of-state tables for astrophysical applications. *Astrophys. J.* **456**, 902 (1996)
- Salpeter, E.E.: Electrons screening and thermonuclear reactions. *Aust. J. Phys.* **7**, 373–388 (1954)
- Saumon, D., Chabrier, G., van Horn, H.M.: An equation of state for low-mass stars and giant planets. *Astrophys. J. Suppl. Ser.* **99**, 713–741 (1995)
- Schlattl, H.: The Sun, a laboratory for neutrino- and astrophysics. Ph.D. thesis, Technical University München (1999)
- Schlattl, H.: Microscopic diffusion of partly ionized metals in the Sun and metal-poor stars. *Astron. Astrophys.* **395**, 85–95 (2002)
- Schlattl, H., Salaris, M.: Quantum corrections to microscopic diffusion constants. *Astron. Astrophys.* **402**, 29–35 (2003)
- Schlattl, H., Weiss, A., Ludwig, H.-G.: A solar model with improved subatmospheric stratification. *Astron. Astrophys.* **322**, 646–652 (1997)
- Spaeth, H.: Spline-Algorithmen zur Konstruktion glatter Kurven und Flächen. Oldenburg, München (1973)
- Swamy, K.S.K.: Profiles of strong lines in K-dwarfs. *Astrophys. J.* **145**, 174–194 (1966)
- Thomas, H.-C.: Sternentwicklung VIII. Der Helium-Flash bei einem Stern von 1.3 Sonnenmassen. *Z. Astrophys.* **67**, 420–455 (1967)
- Thoul, A.A., Bahcall, J.N., Loeb, A.: Element diffusion in the solar interior. *Astrophys. J.* **421**, 828–842 (1994)
- Wagenhuber, J.: Entwicklung von sternern verschiedener massen und metallizitäten auf dem asymptotischen riesenast und danach. Ph.D. thesis, Technical University Munich (1996)
- Wagenhuber, J., Weiss, A.: Numerical methods for AGB evolution. *Astron. Astrophys.* **286**, 121–135 (1994)
- Weiss, A.: Evolutionary models for R CrB stars. *Astron. Astrophys.* **185**, 165–177 (1987)
- Weiss, A.: The progenitor of SN 1987A—uncertain evolution of a 20 solar mass star. *Astrophys. J.* **339**, 365–381 (1989)
- Weiss, A.: Calculation and application of low-mass stellar models. Habilitationsschrift. Universität München (1999)
- Weiss, A., Schlattl, H.: Age–luminosity relations for low-mass metal-poor stars. *Astron. Astrophys. Suppl. Ser.* **144**, 487–499 (2000)